Further insight into the gas flame acceleration mechanisms in pipes. Part II : Numerical work

Guillaume Lecocq, Emmanuel Leprette, Jérôme Daubech, Christophe Proust

Further insight into the gas flame acceleration mechanisms in pipes. Part II: numerical work

Guillaume Lecocq [a], Emmanuel Leprette [a], Jérôme Daubech[a] & Christophe Proust[a,b]

E-mail: *Guillaume.lecocq@ineris.fr*

[a] Institut National de l'Environnement Industriel et des Risques, Parc Technologique ALATA, BP 2, 60550 Verneuil-en-Halatte, France
[b] Sorbonne Universités, UTC-TIMR, 1 rue Dr Schweitzer, 60200 Compiègne, France

Abstract

This paper is the second part of a global study investigating the physics of premixed flame propagation in several kinds of long pipes. It focuses on the potential of CFD for modelling such cases. Four tests among the database detailed in the first part are selected. In each case, the pipe is straight, open at one end and closed at the other where ignition is triggered. The pipe is filled with a stoichiometric methane/air mixture at rest. The parameters which are varied are the inner pipe diameter and the pipe material.

CFD computations based on a URANS framework are carried out and enable to recover several physical trends, such as the role of acoustics and boundary layer turbulence on the flame dynamics. Although most orders of magnitude of the measured overpressure peaks can be predicted numerically, the computed flames are quicker than the measured ones. It could be explained by the chosen turbulent model, the k-ω SST model, known to be adapted for wall-bounded flows but to produce too much turbulence for accelerating flows. The criterion for the cells size near wall (y^+<200) might also be too loose.

Keywords: *premixed flame, methane, pipe, CFD*

1. Introduction

Recent studies (Daubech, 2018) have been carried out to measure pressure signals and flame speed histories for a set of deflagrations occurring in long straight pipes with an open end for varying diameters and materials. These tests highlighted the influence of:

- The acoustics in smooth pipes;
- the nature of the pipe and potentially the influence of the roughness of the wall on the flow.

The oscillatory behaviour of flames propagating in long pipes was previously observed (Guénoche, 1964, Kerampran, 2000) and recovered with models assuming one-dimensional flames and small propagation speed compared to the speed of sound (Fachini, 2004).

Nevertheless, to the authors' knowledge, no single engineering model has been able to predict all the trends mentioned above. It is a challenge as such models are developed by simplifying the full set of equations theoretically describing the deflagration. In this process, effects influencing the flame dynamics such as the three-dimensional topology, the impact of geometrical details and coupling between physical phenomena can be easily lost.

Computational Fluid Dynamics (CFD) can theoretically provide a general model as it can account for all the required physics provided that proper modelling choices are made.

Turbulence in particular can be addressed in several ways in the codes: it can be totally resolved by some lab codes (Moureau, 2011), modelled with the RANS/URANS frameworks as it has been done for many years for industrial designs (Cornejo, 2018) or partially resolved with LES (Urbano, 2017) which is an increasing trend. Mixed RANS/LES techniques were also proposed (Makowka, 2017). For each framework, several combustion models have been proposed by the scientific community. Nevertheless, although the highest resolution of the physics is wanted, it implies large computing power, which is not always available for the modeller.

To the authors' knowledge, deflagrations in long pipes with no obstacles have rarely been investigated with CFD. Such configurations are among the most challenging premixed flame modelling cases. The flame is not stabilized and during its propagation a complex physics impacts its velocity.

The current paper aims at providing the industrial risk engineer with new contributions in the goal of answering the following questions:

- Is it possible to recover the experimental flame speed history and pressure profile for such cases with CFD?
- What could be the accuracy of CFD?
- What is the price to pay by the modeller for getting accurate results? A higher resolution of the physics by the grid, implying more computational power? Or proper modelling choices for turbulence and/or combustion among the bibliography?

Towards this goal, the paper first describes the identified set of experiments, then presents the adopted modelling strategy and finally details the comparison of the predicted flame speeds and overpressure with the measured ones.

2. Cases of interest

The paper focuses on some experiments described in a previous study (Daubech, 2018). In each case, the pipe is straight, 24-m long, open at one end and closed at the other. It is filled with a quiescent stoichiometric methane/air mixture. The mixture is ignited in the centre of the closed end of the pipe with an electrical spark whose energy is about 100 mJ.

Four tests are modelled, for varying pipe inner diameter and material. These tests, as well as the methods employed for measuring pressure and flame speed are summed up in the Table below. Figure 1 shows some of the studied pipes.

Table 1: Selected pipe deflagration tests.

Inner diameter	Material	Pressure probe locations (from ignition point)	Flame tracking method (distances are considered from ignition point)
250 mm	PMMA	0 m, 5 m, 15.5 m	High-speed camera and video processing
	Steel	0 m, 5.4 m, 15.8 m	Photovoltaic cells at: 1.5 m, 8.1 m, 11.9 m and 19.7 m
150 mm	PMMA	0 m, 5.4 m, 15.5 m	High-speed camera and video processing
	Steel	0 m, 5 m, 15.5 m	Photovoltaic cells at: 0.5 m, 5.5 m, 10.5 m and 15.5 m

These tests are attractive for the modeller as methane flames are quite easy to model compared with other hydrocarbons or hydrogen. The tendency of self-instabilities production related to non-unitary Lewis number effects is moderate for methane flames. The geometry is also simple, enabling to rely on a high-quality mesh, reducing the impact of numerics. Furthermore, the sensitivity of two parameters from a reference case is studied

Figure 1: View of the experimental set-up. Top: PMMA pipe, with a 250-mm inner diameter. Bottom: metal pipe, with a 150-mm inner diameter.

3. Modelling strategy

3.1 Physical models

The CFD model has to account for a premixed flame whose propagating speed may not satisfy low Mach number assumptions and can be driven by acoustics, flow curvature and turbulence generation at the walls. For the sake of simplicity, a URANS approach is chosen for modelling turbulence. Indeed, performing a LES is more demanding as it requires a mesh that solves a large part of the total kinetic energy (Pope, 2004).

The Favre-averaged transport equations of pressure, momentum, energy, chemical species and progress variable are solved numerically by the OpenFoam code (Weller, 1998), version 3.0.0. The solver is compressible and solves the acoustics.

Turbulence is modelled with the k-ω SST model (Menter, 2003), commonly chosen for wall-bounded flows. A known drawback of this model nevertheless is that it can produce large turbulence levels in regions with strong accelerations (Fouladi, 2016). This is potentially the case for the flames propagating in pipes.

The chemistry is addressed with a one-step reaction and only methane, oxygen, nitrogen, carbon dioxide and water mass fractions are transported.

Turbulent premixed flame can be modelled with a flame surface-density ($\bar{\Sigma}$) approach. This quantity is approximated as $\Xi|\nabla\tilde{c}|$, where Ξ is the wrinkling factor of the flame related to flame/turbulence interaction and $\tilde{c}$ is the Favre-averaged progress variable. The chemical source terms appearing in the transport equations of the Favre-averaged progress variable and chemical species mass fractions can be closed as (Lecocq, 2011):

$$\bar{\rho}\widetilde{\omega_c} = \rho_u S_L \Xi |\nabla\tilde{c}|$$

$$\bar{\rho}\widetilde{\omega_{Y_i}} = \bar{\rho}\widetilde{\omega_c}(Y_i^b - Y_i^u)$$

Where ρ_u is the volume mass of the fresh gases, $S_L$is the laminar flame speed, Y_i^b (resp. Y_i^u) is the burnt (resp. fresh) gases mass fraction of the i-th chemical species.

The wrinkling factor of the flame is closed algebraically as:

$$\Xi = 1 + \left(1 + 2\Xi_{shape}(c - 0.5)\right)\Xi_{coeff}\sqrt{\frac{u'}{S_L}}R_\eta$$

Where Ξ_{shape} and Ξ_{coeff} are parameters set to 1 and 0.2, c is the progress variable, u' is the fluctuating speed and R_η equals $u'/\left(\epsilon\tau_\eta\right)^{0,5}$ where ϵ is the turbulence dissipation rate. ${\tau_\eta}^2 = (\nu/\rho_u\epsilon)$ with ν, the kinematic viscosity. It was checked before CFD runs (not shown) that the correlation for Ξ gave satisfying results when compared with experiments in which turbulence interacts with methane/air flames (Liu, 2012).

3.2 Computational domain and grid

The computational domain is limited to the part of the pipe filled by the flammable mixture. At walls, velocity is zero and turbulent viscosity is modelled with a wall law. At the outlet plane, the pressure is set to the atmospheric pressure and the velocity gradient is set to 0.

In all cases, the thermal impact of the material is neglected and walls are assumed to be adiabatic (temperature gradient set to 0). The PMMA is assumed to be perfectly smooth and the steel roughness is assumed to be around 150 μm which corresponds to a weakly rusted steel. The turbulent boundary layer is theoretically divided into three parts: a viscous sub-layer close to the wall, an intermediate buffer sub-layer and a logarithmic sub-layer. This latter can be modelled with the following equation: $u^+ = 1/\kappa \ln(Ey^+)$. It relates u^+ and y^+, the normalized flow velocity and distance to the closest wall. κ is the Von Karman constant (0.41) and E is a constant set to 9.8. The previous equation is valid for smooth walls only. In OpenFoam, another boundary condition is proposed for rough walls. It relies on a change of the parameter E in the previous wall law with the chosen wall roughness.

Different grids are used, each one being characterized by a number of cells. For each pipe, the reference mesh is made of 1.4 million cells. The fine mesh is made of 2.5 million cells. The very fine mesh for the 150 (resp. 250) mm pipe contains 4.3 (resp. 6.0) million cells. All grids are composed of hexahedra only, with a characteristic size decreasing from pipe centre to the walls.

The computations are performed for a given case with the reference mesh. The logarithmic sub-layer assumption is valid for values of y^+ ranging roughly between 30 and 200. If this criterion is not fulfilled during the computation of the flame propagation, a finer grid is used for a new computation of the case.

3.3 Computing resources

The computations were run in parallel on several cores of a supercomputer. The computations times were about 10 hours for 1s of physical time with 256 2.4 GHz Intel Xeon cores.

4. Results

4.1 250 mm pipes

4.1.1 The PMMA pipe

A classic way to study flame propagation is to plot the flame position versus time. The numerical flame position is the distance on the pipe axis between the close end and the cell where the progress variable equals 0.5.

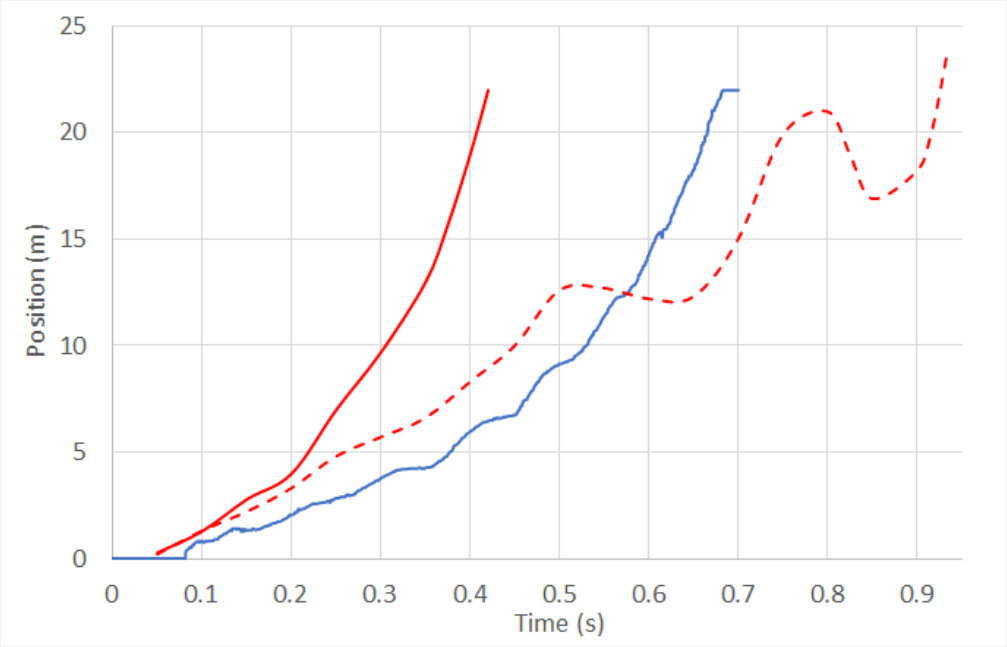

Figure 2: History of the flame front position obtained from the video post-processing (blue), the computations with (red straight line) and without (red dotted line) modelled turbulence.

The comparison between histories of flame positions (Figure 2) shows a numerical flame that propagates on average about 60% quicker than the measured one. Another computation was performed with no modelled turbulence and Ξ set to 1 to investigate these gaps. The laminar and the turbulent numerical flames propagate at the same speed from 0 to 0.2 s, which is too high compared to the experiment. It could be partly explained by the chemical model: the temperature of the burnt gases in the code is about 2600 K, whereas theoretical adiabatic flame temperature at constant pressure is about 2230 K, according to a Gaseq computation (Morley, 2005). Such a gap indeed leads to an overestimation of the expansion rate of the burnt gases which in turn artificially boosts the flame speed. The overestimation is about 20 %. A solution could be to add species like H_2 and CO in the burnt gases composition to improve the temperature prediction.

At a time of about 0.2 s, the turbulent flame strongly accelerates whereas the average speed of the laminar flame is roughly the same from 0 to 0.55 s and follows the experimental trend. The laminar flame shows an oscillatory behaviour. The predicted characteristic period is about 0.2 s which is greater than the experimental one, about 0.08 s. From 0.55 s to the end of the laminar flame propagation, the flame goes backwards whereas the experimental flame keeps on moving forward.

Figure 3 details the laminar flame evolution with time. The modelled flame is never purely flat. It is first elongated (0.5 and 0.1 s) and then adopts a tulip shape (from 0.15 to 0.25 s). It is interesting to note that such a phenomenon can be recovered whereas its origin is still a discussion topic in the scientific community (Xiao, 2012). The time needed for an acoustic wave to propagate from the flame front to the open end and to come back is about 0.15 s. The shape change thus appears directly related to flame/acoustics interaction. From 0.25 s to the end of flame propagation, the flame shape changes constantly, switching from a tulip to an elongated shape with characteristic periods. Note the flame shape directly impacts the flame propagation speed because the total fresh gases consumption rate increases with the flame surface. For the turbulent flame (not shown), flame shapes changes occur during the flame

propagation in the first third of the pipe length. For the rest of the propagation, the flame remains elongated. It seems to mean the flame is sensitive to acoustics when it is sufficiently slow.

After 0.5 s, the laminar flame model is no more coherent with the experiment. It may be explained by an acceleration of the flame by turbulence which is not accounted for by the model. It can also be a numerical artifact due to the decreasing distance between the outlet boundary condition and the flame front. Extra computations should be performed by meshing a part of the atmosphere and moving the boundary conditions away from the flame path.

It appears CFD can approach the experimental flame behaviour with a laminar assumption for half the flame propagation length. When turbulence is accounted for, the model overpredict the production rate and/or amount although the walls are assumed to be smooth. It can be due to the turbulence model itself and/or to the criterion on the maximum value of y^+ which could be not constraining enough.

It should be noted that according to the experiment interpretation (Daubech, 2018), turbulence may not play such an important role in the flame propagation history contrary to other phenomena like acoustics. This observation explains why the best numerical agreement is obtained with the laminar flame assumption.

The computed and measured overpressures 15.5 m from ignition point are shown in Figure 4. In coherence with observations from the flame histories, the best results are obtained with the laminar model, in terms of orders of magnitudes for peak overpressures and characteristic periods from 0 to 0.45 s. After this time, the coherence is lost. It is noticeable that even if the turbulent flame propagates too quickly compared to the experiment, the characteristic orders of magnitude for the peak overpressures are predicted. It is maybe due to a balance between a higher pressure production by the flame inducing an enhanced volume flow rate at the outlet plane.

4.1.2 The metal pipe

The turbulent flame model is tested for the metal pipe case.

Figure 5 shows the effect of roughness on the results: from 0 to about 0.2 s, the flame propagation speed is the same for a smooth and a rough pipe. After 0.2 s, the rough pipe flame propagates faster. Again, turbulence seems to be produced too quickly when compared to the experiment. Nevertheless, the quantitative impact of roughness on the average flame speed seems to be recovered by CFD with an increase of about 20 %.

Figure 6 highlights the model recovers the characteristic periods of the overpressure signal despite the peaks are overestimated from 0 to about 0.25s. Even for a flame which seems to be predominantly driven by flame/turbulence interactions, acoustics still play an important role on the overpressure signal.

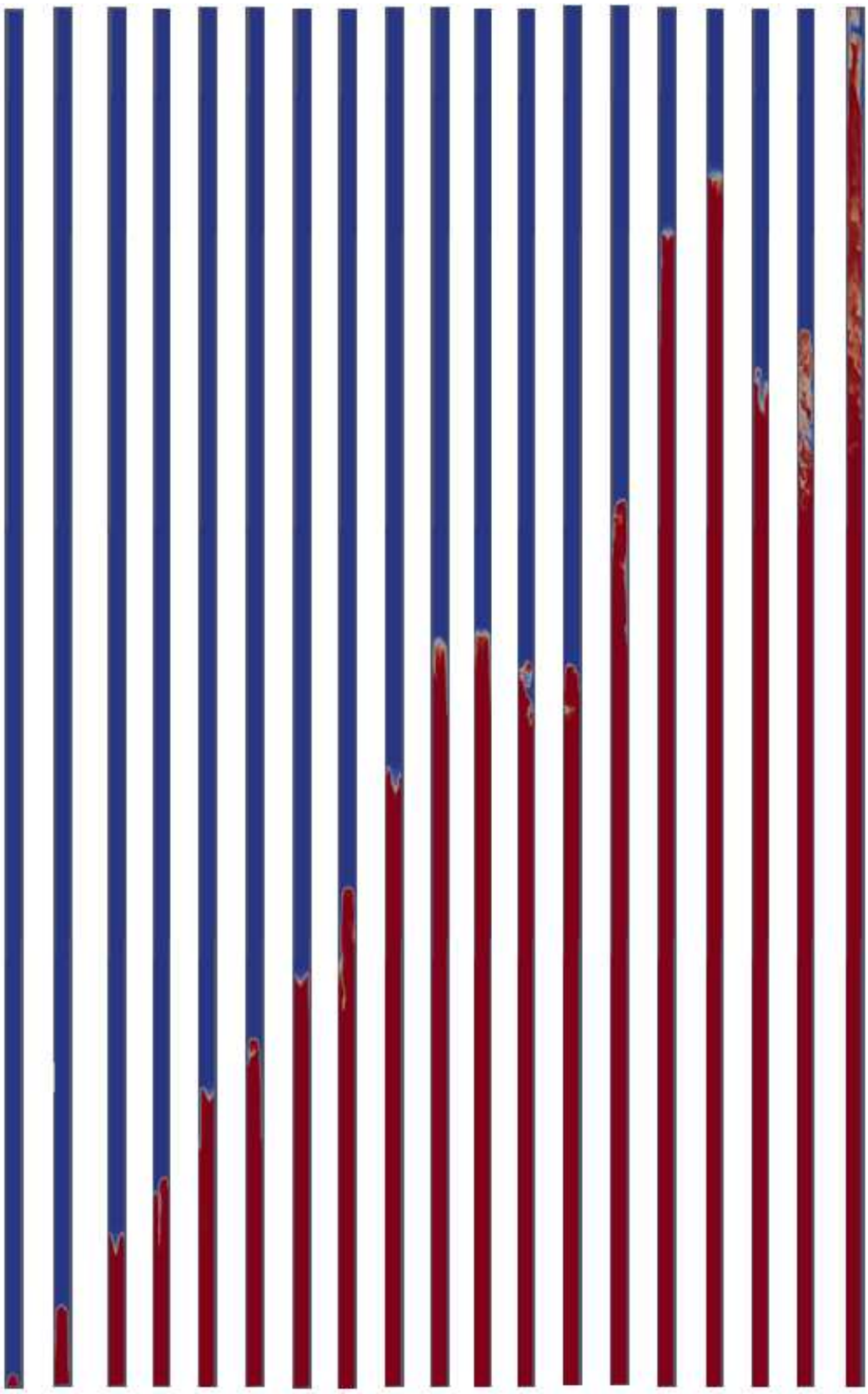

Figure 3: Fields of progress variable (blue: fresh gases, red: burnt gases) ranging from 50 to 950 ms, every 50 ms.

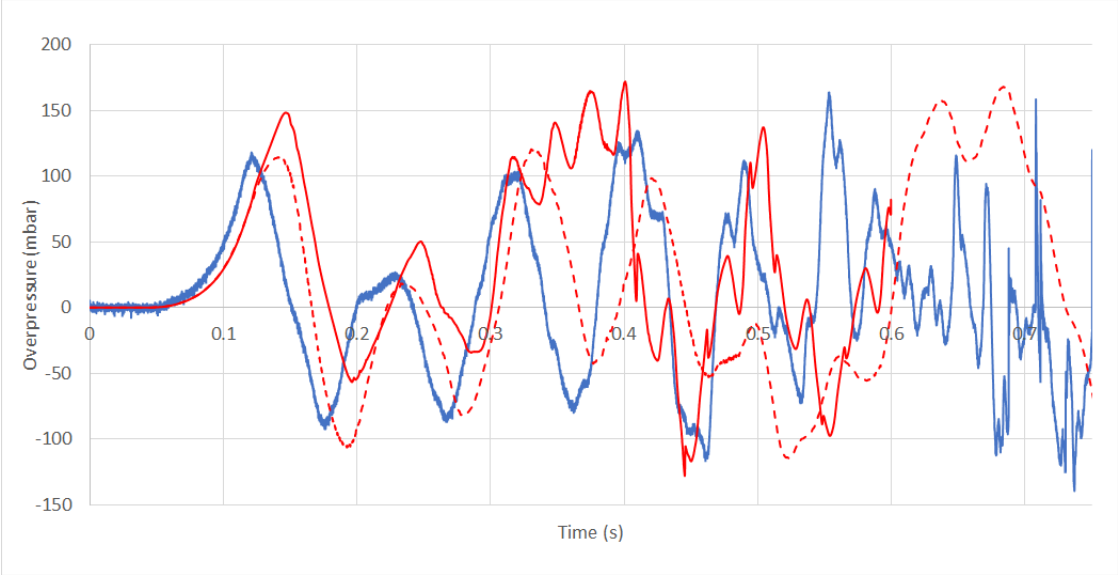

Figure 4: Overpressure signals 15.5 m from ignition point. Case of the 250 mm PMMA pipe. Data from the video post-processing (blue), the computations with (red straight line) and without (red dotted line) a modelled turbulence.

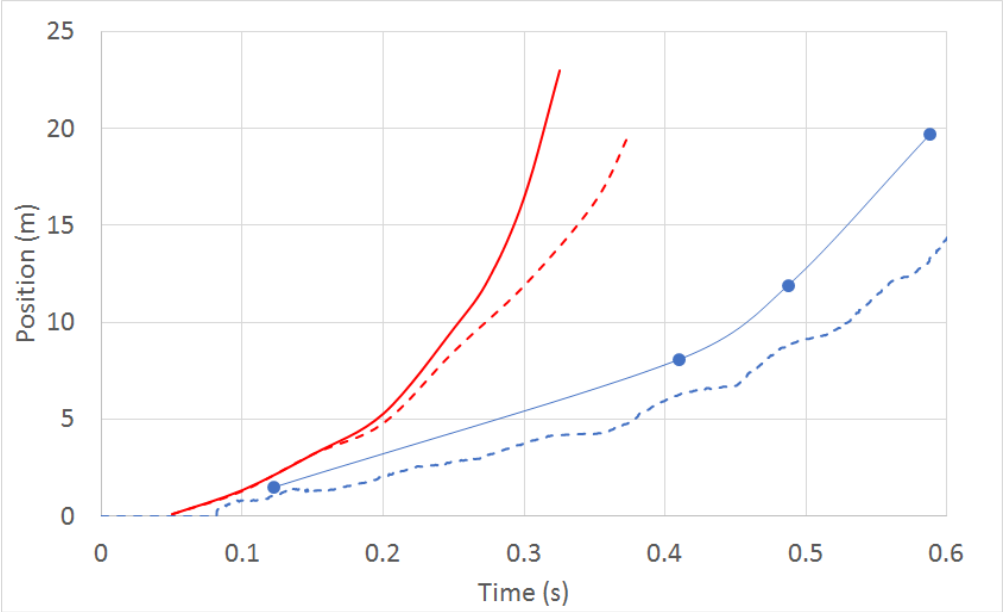

Figure 5: History of the flame front position measured experimentally (blue) and computed with a modelled turbulence (red). Line: metal pipe. Dotted line: PMMA pipe.

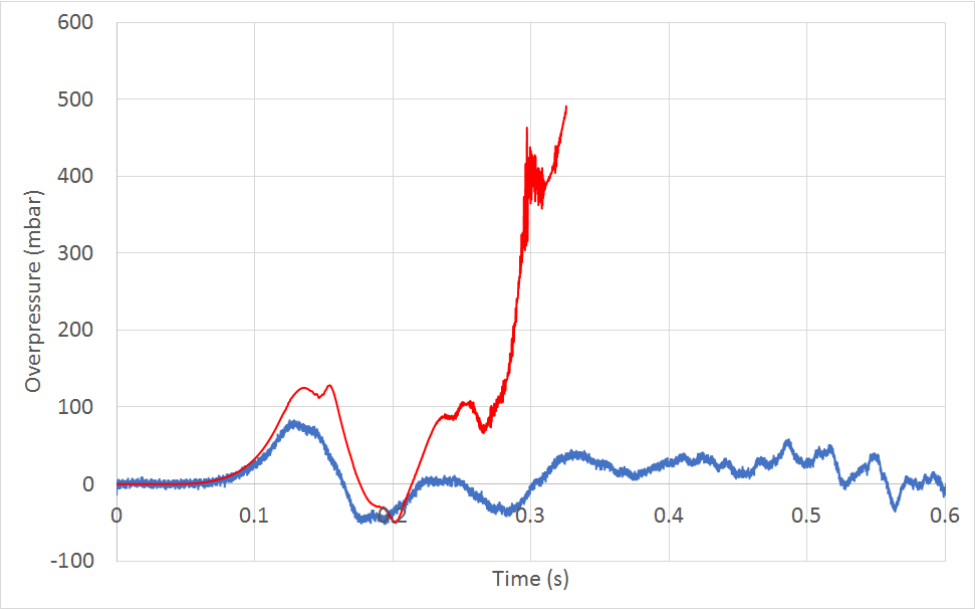

Figure 6: Overpressure signals 15.8 m from ignition point. Case of the 250 mm metal pipe. Data from the video post-processing (blue) and the computation (red).

4.2 150 mm pipes

4.2.1 The PMMA pipe

150 mm pipes are studied to check if the pipe diameter impact on the flame dynamics could be recovered numerically.

For the PMMA pipe, again, two types of models are employed: one with a modelled turbulence, the other with a "laminar" assumption. The position versus time diagram shows (Figure 7) that both models provide the same average flame speed from 0 to 0.7 s with oscillations having the same order of magnitude. This observation is somewhat different from the computation results for the 250 mm PMMA pipe with very different histories if the turbulence is modelled or not. Note it is not possible to compare these results with an experimental diagnostic as several camera positions were tested, giving different reconstructed flame histories through video post-processing.

The experimental overpressure signal (Figure 8) is again best approached by the laminar assumption, in terms of characteristic periods and peaks order of magnitude from 0 to 0.3 s. There is nevertheless a time lag as it appears probable the numerical laminar flame propagates quicker than the experimental flame. As noticed for the 250 mm PMMA pipe, even if the turbulent flame is too quick, correct orders of magnitude are predicted for the overpressure peaks.

4.2.2 The metal pipe

The metal pipe is modelled with the turbulent flame model accounting for roughness effects at the walls. Figure 9 highlights a good agreement between the experimental and numerical

flame position histories. It can be seen the numerical flame accelerates too strongly compared with the experiments at 0.15 s.

The consequences of these observations on the overpressure signals are shown in Figure 10: a good agreement with pressure history from 0 to 0.2 s but maximum overpressures that are twice higher than the experimental ones after 0.2 s.

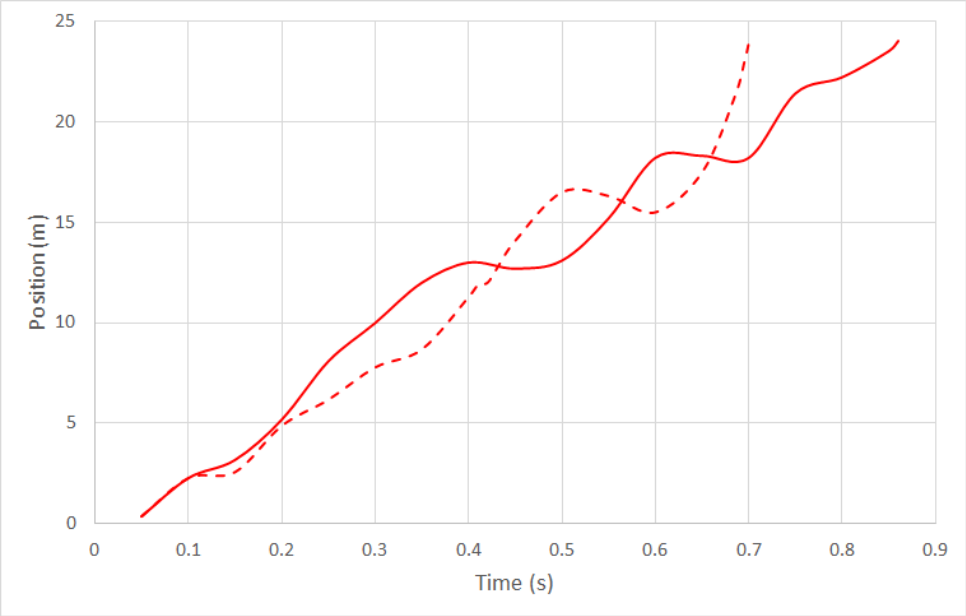

Figure 7: History of the computed flame front position with (line) and without (dotted line) turbulence modelled. Case of the 150 mm PMMA pipe.

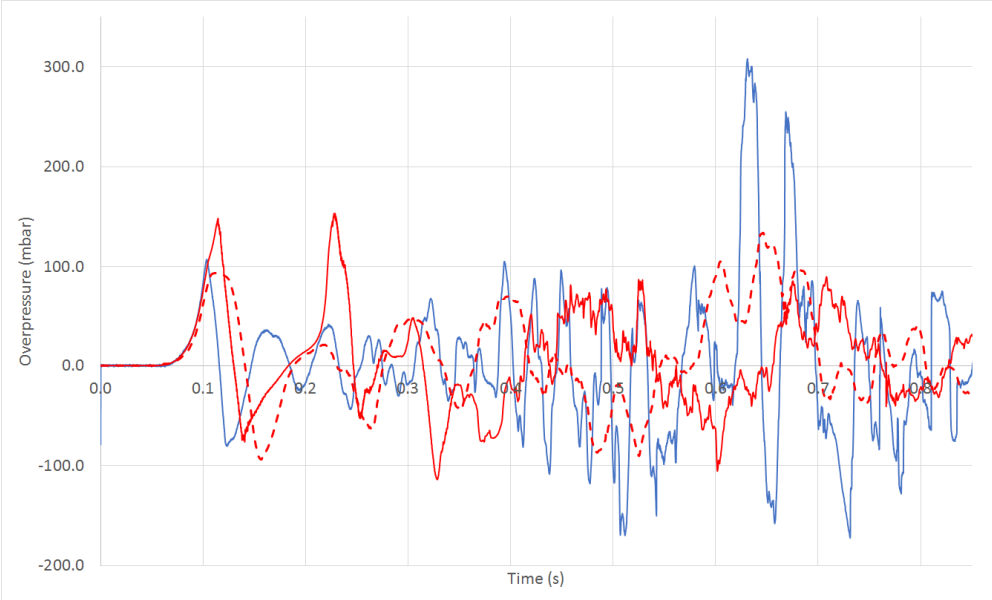

Figure 8: Overpressure signals 15.5 m from ignition point. Case of the 150 mm PMMA pipe. Data from the video post-processing (blue), the computations with (red straight line) and without (red dotted line) a modelled turbulence.

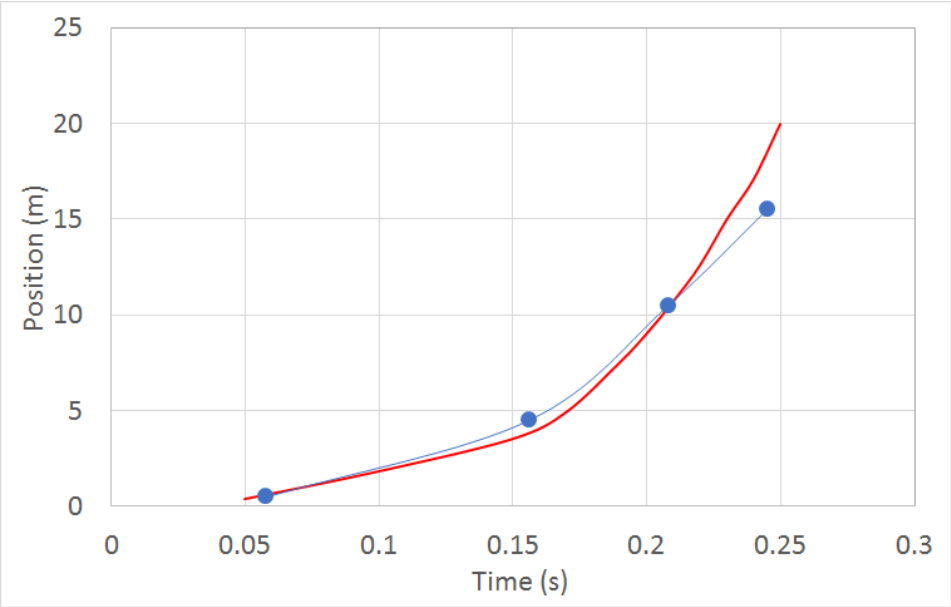

Figure 9: History of the flame front position measured experimentally (blue) and computed (red). Case of the 150 mm metal pipe.

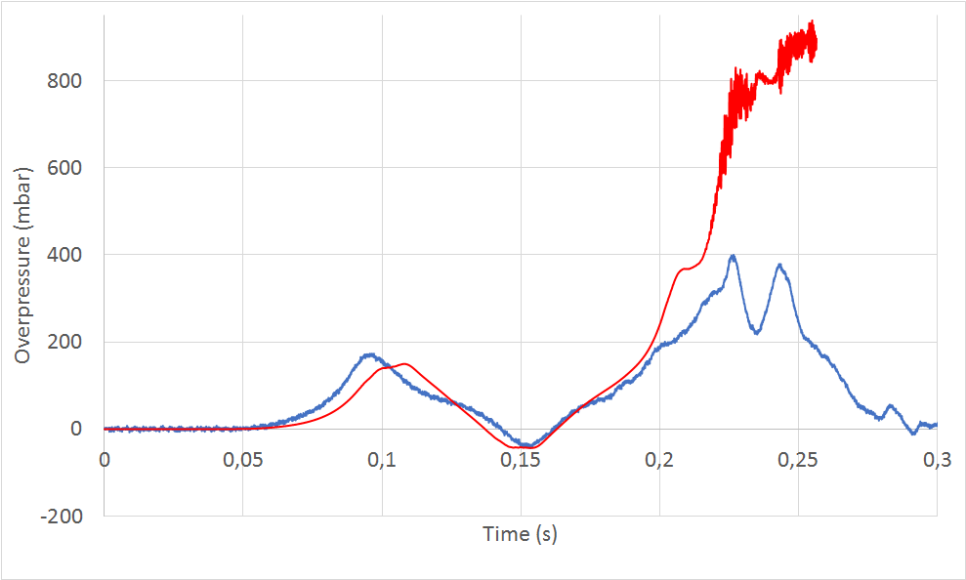

Figure 10: Overpressure signals 15.5 m from ignition point. Case of the 150 mm metal pipe. Data from the photovoltaic cells (blue) and the computations(red).

5. Conclusions

CFD computations were carried out for a set of 24 m long pipes in which initially quiescent, stoichiometric methane/air mixtures were ignited.

The set of compressible equations describing combustion and solving the acoustics was numerically solved with OpenFoam 3.0.0 for four kinds of pipes, with varying materials and diameters.

Even if the numerical results did not perfectly match the experimental measurements and some modelling aspects such as chemistry and the interaction of pressure waves with the atmosphere should be improved, they enabled to give first answers to the following questions:

- *Is it possible to recover with CFD the experimental flame speed history and pressure signals for such cases?* The results showed the capacity of CFD to recover many trends of the phenomena related to premixed flame propagation in pipes: flame shape changes, flame/acoustics coupling, flame acceleration related to rough walls, …
- *What could be the accuracy of CFD*? Orders of magnitude for the pressure peaks were most of the time recovered. Acceleration may have been under/overestimated due to the turbulence model and/or the modelling of turbulence at walls. Maybe better results could be obtained with a maximum y^+ value lower than 200.
- *What is the price to pay by the modeller for getting accurate results? A higher resolution of the physics by the grid, implying more computational power? Or proper modelling choices for turbulence and/or combustion among the bibliography?* The URANS approach could theoretically give better results with another turbulence model. The k-ω SST model is indeed known to produce too much turbulence for accelerating flows. Nevertheless, no other turbulence model was tested in this work.
When the flame accelerates, maximum y^+ values increase ahead of the flame front, requiring a finer mesh at the walls to limit this increase. For the author, the grid fineness constraint in the model is related to wall treatment. This constraint would be even more demanding for fuels prone to lead to higher flame speed such as hydrogen. The obtained URANS meshes could be compatible with the LES technique but this also should be checked.

Acknowledgements

The authors gratefully acknowledge the financial contribution granted by the Research Fund for Coal and Steel (RFCS) for the EXPRO project during which the presented computations were performed.

References

Daubech, J., Proust Ch., Leprette E. & Lecocq G. (2018). *Further insight into the gas flame acceleration in pipes. Part I: experimental work*. International Symposium on Hazard, Prevention and Mitigation of Industrial Explosions, 12 (submitted).

Guénoche H. (1964). *Nonsteady flame propagation*. Markstein (Ed.), Pergamon Press.

Kerampran S., Desbordes D. & Veyssière B. (2000). *Study of the Mechanisms of Flame Acceleration in a Pipe of Constant Cross Section*. Combustion Science and Technology, 158: 71-91.

Fachini F.F. & Bauwens L. (2013). *Oscillatory flame propagation: Coupling with the acoustic field*. Proceedings of the Combustion Institute, 34: 2043-2048.

Moureau V., Domingo P. & Vervisch L. (2011). *From Large-Eddy-Simulation to Direct Numerical Simulation of a lean premixed swirl flame: Filtered laminar flame PDF modelling*. Combustion and Flame 158(7): 1340-1357

Cornejo I., Niktrityuk P. and Hayes R.E. (2018). *Multiscale RANS-based of the turbulence decay inside of an automotive catalytic converter*. Chemical Engineering Science, 175: 377-386

Urbano A., Douasbin Q., Selle L., Staffelbach G., Cuenot B., Schmitt T., Ducruix S. & Candel S. (2017). *Study of flame response to tranverse acoustic modes from the LES of a 42-injector rocket engine*. Proceedings of the Combustion Institute, 36: 2633-2639.

Makowka K., Dröske N.C., Von Wolfersdorf J. & Sattelmayer T. (2017). *Hybrid RANS/LES of a supersonic combustor*. Aerospace Science and Technology, 69: 563-573.

Pope S.B. (2004). *Ten questions concerning the large-eddy simulation of turbulent flows.* New Journal of Physics, 6: 35.

Weller H.G. & Tabor G. (1998). *A tensorial approach to computational continuum mechanics using object-oriented techniques*. Computational Physics, 12: 620-631.

Menter F.R., Kuntz M., and Langtry R. (2003). *Ten years of industrial experience with the SST turbulence model*. Proceedings of the international symposium on turbulence, heat and mass transfer, 4: 625–632.

Fouladi K. (2016), *Elements of Turbulence Modeling*, NAFEMS World Congress

Lecocq G, Richard S., Colin O. & Vervisch L. (2011). *Hybrid presumed pdf and flame surface density approaches for Large-Eddy Simulation of premixed turbulent combustion Part 1: Formalism and simulation of a quasi-steady burner*, Combustion and Flame 158: 1201-1214

Liu C.C., Shy S.S., Peng M.W. & Dong Y.C. (2012). *High-pressure burning velocities measurements for centrally-ignited premixed methane/air flames interacting with intense near-isotropic turbulence at constant Reynolds numbers*, Combustion and Flame, 159: 2608-2619

Morley C. (2005). *Gaseq*. http://www.gaseq.co.uk/

Xiao H., Makarov D., Sun J. and Molkov V. (2012). *Experimental and numerical investigation of premixed flame propagation with distorted tulip shape in a closed duct*. Combustion and Flame, 159(2) : 1523-1538.